

Electroless Pd deposition on a planar porous stainless steel substrate using newly developed plating rig and agitating water bath

Beom-Seok Seo^{*,**}, Jae-Yun Han^{*}, Kwan-Young Lee^{**,†}, Dong-Won Kim^{***}, and Shin-Kun Ryi^{*,†}

^{*}Advanced Materials and Devices Laboratory, Korea Institute of Energy Research (KIER),
152 Gajeong-ro, Yuseong-gu, Daejeon 34129, Korea

^{**}Department of Chemical and Biological Engineering, Korea University, 5-Ga, Anam-dong, Sungbuk-gu, Seoul 02841, Korea

^{***}Department of Advanced Materials Engineering, Kyonggi University, Suwon, Gyeonggi-do 16227, Korea

(Received 5 July 2016 • accepted 5 September 2016)

Abstract—A new plating bath was developed to prevent palladium plating in the pores of the porous stainless steel support when using plate-type porous substrate. The plating bath, composed of a holder, a rubber O-ring and a bottom, provides very simple assembly and is very effective in preventing palladium plating in the pores of porous stainless steel. The agitation of the plating solution increases plating rate significantly because the agitation improves the external mass transfer of Pd ion and reducing agent to the membrane surface facilitating ~99.7% plating yield of palladium ion. This new plating method carried out at a temperature range of 293 to 298 K provides a very simple and economic membrane manufacturing process. Using a newly developed plating rig, an 88.9-mm diameter membrane was fabricated, and gas permeation tests showed that the hydrogen permeation flux reached $\sim 0.9 \text{ mol s}^{-1} \text{ m}^{-2}$ at 873 K and a pressure difference of 300 kPa and selectivity (H_2/N_2) was $\sim 1,850$ at 873 K with a pressure difference of 100 kPa.

Keywords: Pd Membrane, Hydrogen, Electroless Plating, Porous Stainless Steel, External Mass Transfer

INTRODUCTION

Pd-based membranes can selectively transport hydrogen and have attracted considerable interest in their use in hydrogen separation and production devices [1-3]. Several review articles provide a thorough perspective on developments and applications of the Pd-based hydrogen selective membranes [4-6]. The approach of composite structure, which consists of a porous substrate and a thin membrane layer, provides the obvious advantages of decreased membrane thickness, increased hydrogen permeation flux, reduced material costs and easy modulation for industrial applications. Materials that have been used for porous substrates include ceramics, glass and metals such as stainless steel, Inconel, nickel and Hastelloy [7]. Electroless plating (ELP) is the most attractive method for coating Pd on porous substrates over other techniques, including sputtering, chemical vapor deposition (CVD), electroplating and spray pyrolysis because of its relative simplicity, low cost, hardness of deposits, flexibility, good adhesion to the substrate and ease of scaling up [8,9]. Despite its advantages, ELP suffers from low deposition rate, metal loss and film impurities [10].

ELP of Pd is based on the reduction of palladium ion on an activated substrate assisting reducing agent [11]. The microstructure of Pd film has an important effect on the permeation properties,

such as permeation flux and selectivity [12]. The plating rate is dependent on temperature and the concentration of Pd ion and reducing agents, usually N_2H_4 , and the microstructure and quality of the Pd layer depends on the plating rate. A high plating rate resulted in non-uniformity of the Pd layer and poor selectivity [13-15]. To obtain higher selectivity, ambient temperature ELP has been reported by Nair et al. [13], Ilias et al. [16] and Govind and Atnoor [17]. In a previous study, Grace's group and Ryi developed ambient temperature ELP using an EDTA (ethylenediaminetetraacetic acid)-free bath to prevent impurity deposition coming from EDTA [7]. The problem of ambient temperature ELP is that a long duration is required for sufficient palladium ion usage. The environmental concerns must be considered after ELP process for the used solution. To develop an environmentally friendly process, it is very important to treat, minimize and recycle the waste plating solution. Moreover, for the commercially application, mass-production is very important.

Therefore, we focused on 1) increasing mass transfer of Pd ion and reducing the plating duration typically observed in ambient temperature ELP for Pd-based composite membrane, 2) maximizing the plating yield to avoid metallic contaminants (Pd) recovery and minimizing waste treatment cost, and 3) developing plating rig for mass production and avoiding palladium deposition in the pores of a planar metal support during electroless palladium plating using an EDTA-free bath. In a previous study, the bottom of the ceramic-modified planar porous stainless steel (PSS, Mott, 0.5 μm grade, 50.8 mm diameter) was shielded by palmitic acid prior to palladium plating [18]. To skip shielding the bottom of the substrate and removing the shielding material, i.e., palmitic acid, a new plating rig, which is composed of a holder, a rubber O-ring, a bot-

[†]To whom correspondence should be addressed.

E-mail: h2membrane@kier.re.kr, h2membrane@gmail.com,
kylee@korea.ac.kr

[‡]This article is dedicated to Prof. Sung Hyun Kim on the occasion of his retirement from Korea University.

Copyright by The Korean Institute of Chemical Engineers.

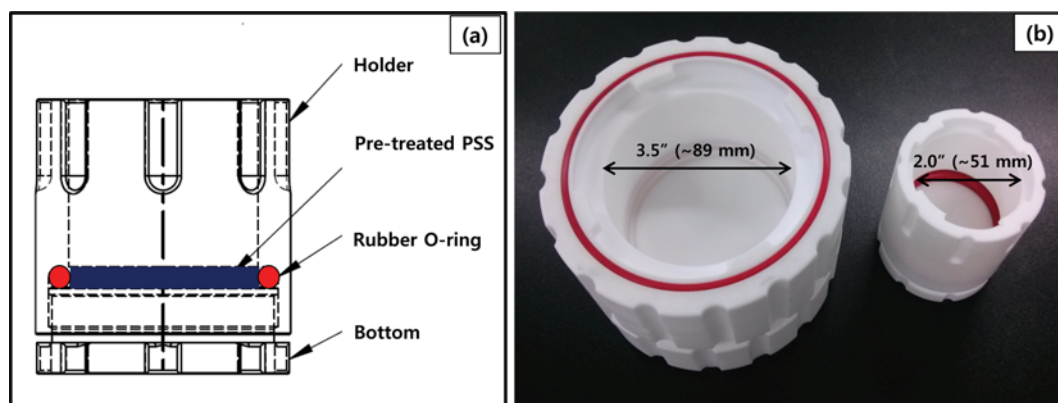


Fig. 1. Schematic of newly developed plating bath (a) and their photos (b).

tom and a stopper, was developed as shown in Fig. 1. The plating rig equipped with a pre-treated planar porous stainless steel (PSS) substrate was shaken using a temperature- and rpm-controllable water-bath. Plating yield was determined by the weight gain method and compared with the conventional method. Hydrogen permeation and nitrogen leak tests were then conducted at temperatures in the range of 673 to 873 K, with a pressure difference of 100-500 kPa.

EXPERIMENTAL

Palladium membranes were synthesized on pre-treated porous stainless steel (PSS) discs with an 88.9-mm diameter and a 1.2-mm thickness (Mott, 0.5 μm grade). The pre-treatment of the PSS included micron-sized ceramic powder filling, submicron-sized ceramic power filling and nano-sized diffusion barrier coating using the method shown in previous studies [7,18,19]. To fill the large size entrance pores of PSS, 5 μm ZrO_2 powder was used in this study. A 50-nm yttrium stabilized zirconia (YSZ) powder, which was for the diffusion barrier between Pd and PSS, was coated by the screen printing method using 8 mol% YSZ paste (KCeraCell Co., Ltd., 17 wt% solid weight paste). After heat-treatment at 923 K for 2 h, the YSZ-coated PSS was seeded with Pd nuclei using the method shown in a previous study [7]. The pre-treated PSS was mounted on the plating rig shown in Fig. 1. The assembled plating rig was filled with an 81 ml EDTA-free plating solution, whose composition was provided in a previous study [7], and then plating was performed and repeated three times. During the Pd plating, the plating rig was shaken at an RPM of 100 using the temperature controllable water bath shown in Fig. 2. The water bath was lab-scale and was designed to manufacture six membranes with an 88.9-mm at the same time. The ratio of the plating solu-

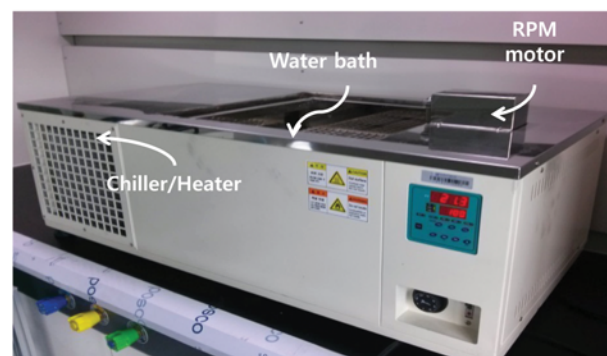
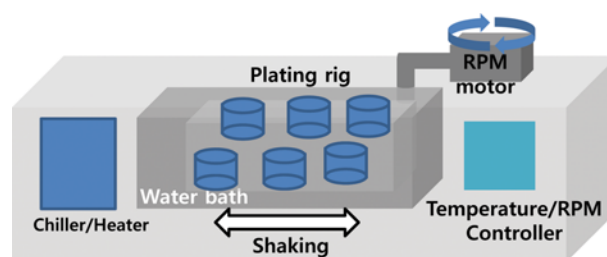


Fig. 2. Temperature- and RPM-controllable water bath for electroless plating.

tion volume to the membrane surface area was $\sim 1.3 \times 10^{-3} \text{ L cm}^{-2}$, which is similar to the previous studies [7]. The influence of plating temperature on membrane morphology, plating rate and plating yield was tested between 293 and 298 K using pre-treated PSS discs with a 50.8-mm diameter and a 1.2-mm thickness (Mott, 0.5 μm grade). The designation of the membranes is in Table 1.

The morphology was characterized by SEM, and plating yield was calculated by the weight gain method using the following equa-

Table 1. Preparation condition of the membranes

| Membrane | Outer diameter [mm] | Area [$\times 10^{-3} \text{ m}^2$] | Plating temp. [K] | Shaking speed [rpm] | Plating times | Thickness [μm] |
|-----------------|---------------------|---------------------------------------|-------------------|---------------------|---------------|-----------------------------|
| KIER-Pd-201-20 | 50.8 | 2.0 | 293 | 100 | 4 | 8 |
| KIER--Pd-201-22 | 50.8 | 2.0 | 295 | 100 | 4 | 8 |
| KIER--Pd-201-25 | 50.8 | 2.0 | 298 | 100 | 4 | 8 |
| KIER--Pd-351-20 | 88.9 | 6.2 | 293 | 100 | 3 | 6 |

tion:

$$\text{Pd plating yield} = (\text{gained Pd weight} / \text{Pd weight in the plating solution}) \times 100 \quad (1)$$

The prepared membrane was mounted in stainless steel permeation cells with a metal O-ring as shown in a previous study [20]. Hydrogen permeation and nitrogen leak tests were then conducted in the range of 673 to 873 K, with a pressure difference of 100-500 kPa.

RESULTS AND DISCUSSION

1. Electroless Pd Plating

Electroless plating is considered as the autocatalytic reduction of metal ion with the oxidation of the reductant. Literature results suggest that the plating rate and grain size depend on the temperature [7,9,11,13-15]. Pd plating was continued for 1 h, and the plating rate was determined during that time. Temperature was varied from 293 to 298 K. Fig. 3 shows the effect of plating temperature on plating rate. The plating rate increased with temperature and reached $\sim 1.62 \mu\text{m h}^{-1}$ at 298 K (25 °C). In 1958, Rhoda developed the hydrazine-based electroless Pd plating bath and observed a linear increase in the plating rate within the temperature range of 40 to 80 °C from $3.8 \mu\text{m h}^{-1}$ to $14.7 \mu\text{m h}^{-1}$ at the ratio of the plating solution volume to the substrate surface area of $1 \times 10^{-2} \text{ L cm}^{-2}$ [11]. Nair et al. [13] showed that the plating rate was dependent on the temperature and the reactant concentration and showed a maximum rate of $1.4 \mu\text{m h}^{-1}$ at 23 °C and a ratio of the plating solution volume to the substrate surface area of $2.5 \times 10^{-3} \text{ L cm}^{-2}$. The plating rate depends on the ratio of the plating solution volume to the substrate surface area because the plating rate decreases rapidly with time due to hydrazine decomposition and the decrease of palladium ion with plating time, which means that a higher ratio of the plating solution volume to the substrate surface area results in a faster plating rate. Considering the ratio of the plating solution volume to the substrate surface area, the plating rate of this study is quite high.

The environmental concerns related to the plating solutions used for the ELP must be investigated. Waste ionization includes source

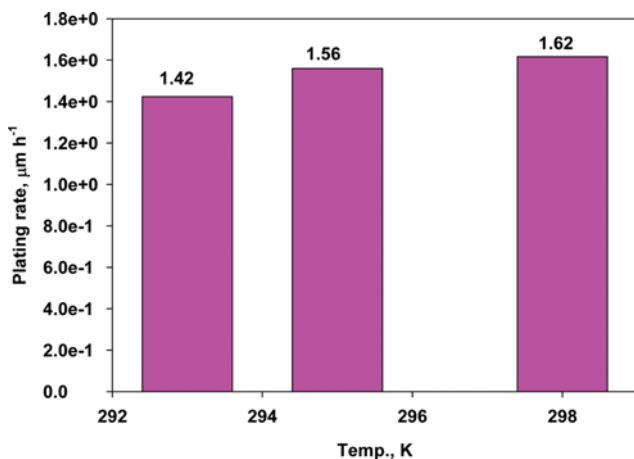


Fig. 3. Pd plating rate as a function of temperature.

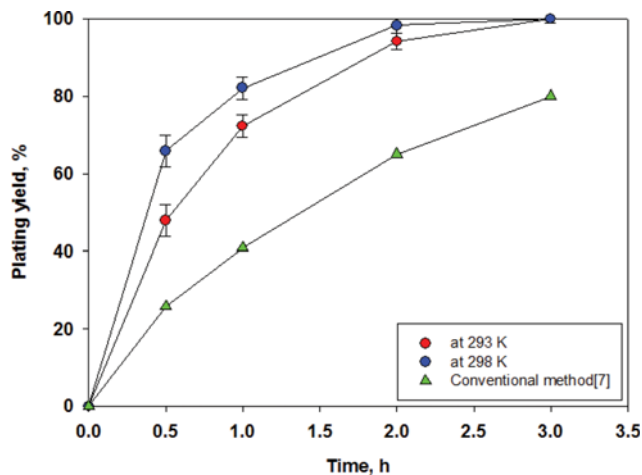


Fig. 4. Plating yield as a function of time: the data of conventional method was from reference [7].

reduction in which the amount of waste is reduced at the source through changes in industrial processes and resource recovery of metallic contaminants prior to discharge to minimize quantities of hazardous waste generated [21]. From the viewpoint of recovery metallic contaminants, plating yield is very important. Fig. 4 shows the plating yield as a function of time. The data of the conventional method was from the previous study [7]. The plating was repeated four times and the plating yield was in the 5% error. It confirmed the reproducibility. The Pd deposition rate usually decreases with plating time due to a decrease of Pd ion concentration and a depletion of reducing agent in the plating solution [13]. During 3 h, the Pd plating yield reached $\sim 80\%$ using the conventional method carried out at 293 K, but almost $\sim 100\%$ Pd was plated with our new plating method at a similar condition. After the Pd plating for 3 h, the plating solution was analyzed with ICP (Inductively coupled plasma, Leeman Lab, PS1000UV Sequential) spectrometry. The remaining Pd in the newly developed method and conventional method was 2.67 ppm and 487 ppm, respectively. It means that $\sim 99.9\%$ of Pd was consumed with the newly developed method, while 79.7% with the conventional method. As the plating reaction takes place on the surface of the membrane, there is the mass-transfer resistance of the Pd ion and the reducing agent.

As described in the introduction, the literature shows that the quality of the Pd film depends on the plating rate. If the plating rate is too fast, the membrane has poor selectivity because the grain size is non-uniform [7,13-15]. They increased the plating rate with the concentration of reductant, i.e., hydrazine, or plating bath temperature. Electroless plating is very sensitive of temperature and reductant. In the previous study [7], non-uniform bulk grains were observed at 308 K but very compact dense film at 293 K. Fig. 5 shows the surface morphologies of membrane KIER-Pd-201-20 (a), KIER-Pd-201-22 (b) and KIER-Pd-201-25 (c). The designation of the membranes is in Table 1. As shown in Fig. 5, the three membranes had similar morphologies with a grain size of 100 nm. The morphologies were very dense and no pinholes were observed on the surface SEM images like the membrane prepared by conventional method [7]. This result indicated that we could increase plating

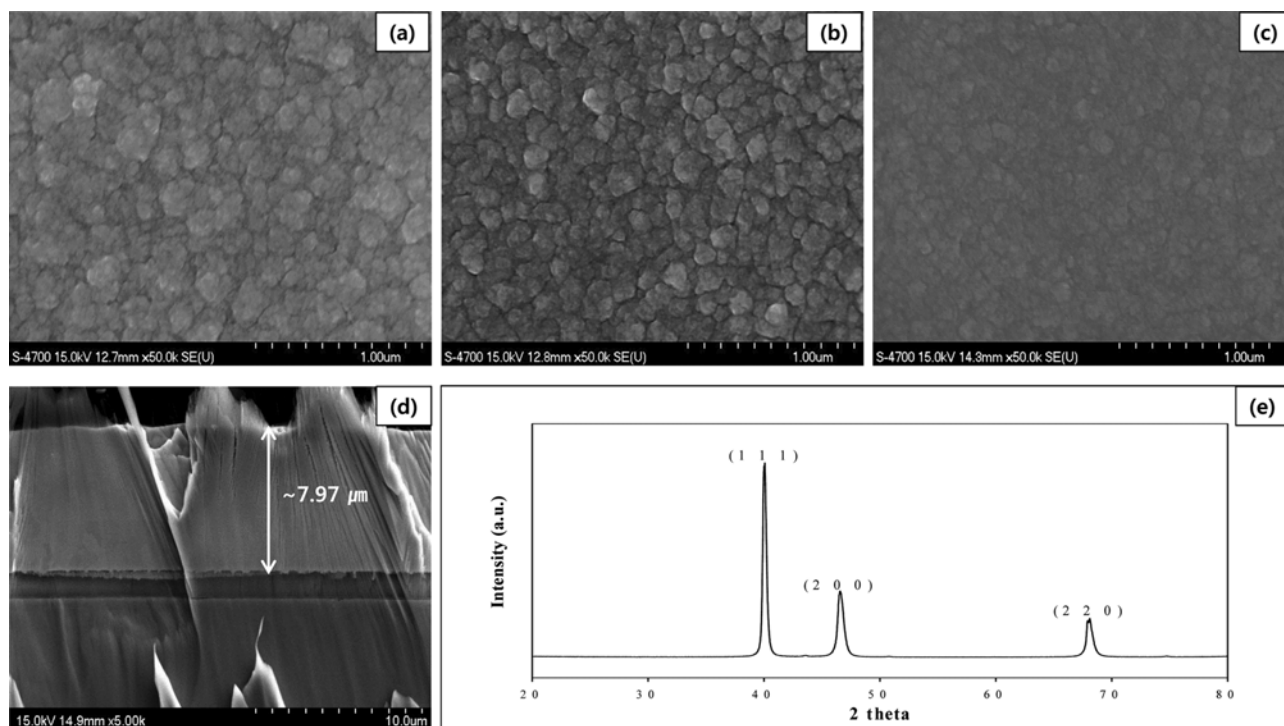


Fig. 5. Surface SEM images of KIER-Pd-201-20 (a), KIER-Pd-201-22 (b) and KIER-Pd-201-25 (c); cross-sectional SEM image of KIER-Pd-201-20 (d); XRD pattern of the fresh membrane fabricated by the same process of KIER-Pd-201-20 (e).

rate with temperature without morphology change in the range of 293 to 298 K, which is a comfortable living condition for human being, so no further equipment for temperature control is required. Therefore, our ambient temperature plating method provides a very simple and economic membrane manufacturing process. The cross-sectional SEM image of KIER-Pd-201-20 in Fig. 5(d) shows that the thickness was $\sim 7.97 \mu\text{m}$. We controlled the plating solution to be $\sim 2 \mu\text{m}$ thick Pd for one-time plating. Plating was repeated four times, indicating the average plating yield was $\sim 99.6\%$.

Some studies show the effect of external mass transfer on the plating rate and deposition morphology. Ayturk et al. [22] reported that the Pd and Ag deposition rate increased by agitating the plating bath for tubular shape membrane. Braun et al. [23] showed that the final thickness of Pd/Ru layer increased with increase of stirring rate and no further effect above 400 rpm. Bulasara et al. [24,25] reported that sonication contributed significantly towards maintaining higher plating efficiency, selective conversation and faster plating rate. However, they have not shown the metallic contaminant after the plating.

In this study, we neutralized the influence of the mass-transfer resistance by shaking the plating bath. The continuous agitation of the plating solution assisted the transfer of Pd ion and the reducing agent to the membrane surface, leading to an increased plating yield and $\sim 99.9\%$ use of Pd in the plating solution to simplify the waste solution treatment. We designed the lab-scale water bath to manufacture six membranes with an 88.9-mm at the same time. It means that our newly developed plating rig and bath provide the possibility of mass-production.

A membrane was fabricated to analyze crystal structure by XRD

with the similar process of KIER-Pd-201-20 XRD, and the XRD pattern is shown Fig. 5(e). The membrane had a predominantly (111) crystal orientation with (200) and (220). Mardilovich et al. [26] observed a similar result from the Pd composite membrane prepared by electroless plating on a PSS.

2. Membrane Stability

Long-term stability test was performed using membrane KIER-Pd-201-20 at 773 K for ~ 260 h. During the long-term durability test period, hydrogen permeation and nitrogen leakage was monitored continuously. The result in Fig. 6 shows that the hydrogen permeation and nitrogen leakage remained stable at ~ 0.22 and $\sim 1.5 \text{ mol s}^{-1} \text{ m}^{-2}$, respectively.

After the long-term stability test, membrane was cooled and cut

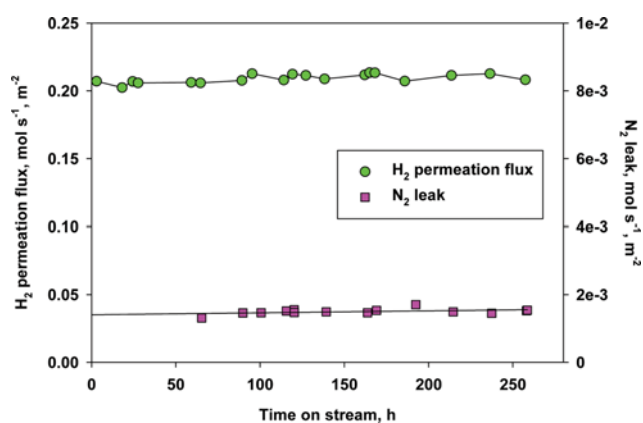


Fig. 6. Long-term stability of membrane KIER-Pd-201-20 at 773 K.

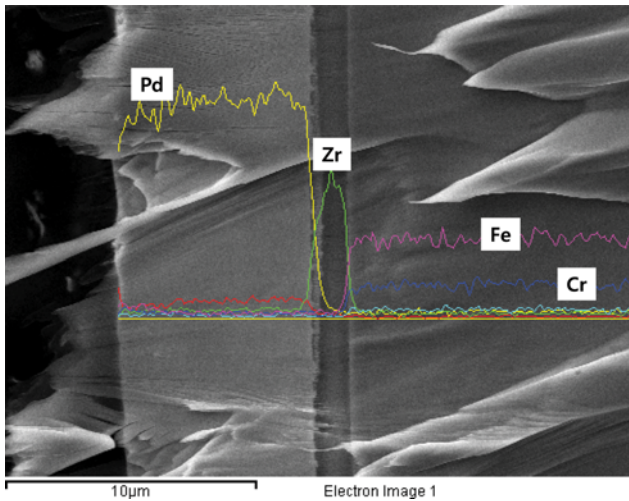


Fig. 7. Cross-sectional SEM image and EDX line-scan profiles of the KIER-Pd-201-20 after long-term stability.

to be analyzed using SEM/EDX. Fig. 7 shows cross-sectional SEM image and EDX line-scan profiles of the KIER-Pd-201-20 after long-term stability. Only one major peak of palladium profiles was observed on top of $\sim 1.5 \mu\text{m}$ of ZrO_2 layer which was deposited as diffusion barrier. This result is similar to the previous study that blocked the bottom of the substrate using palmitic acid [18].

3. Permeation Behavior

A membrane for the hydrogen permeation test was successfully fabricated on pre-treated porous stainless steel (PSS) discs with an 88.9-mm diameter and a 1.2-mm thickness. We fabricated an 88.9-mm diameter membrane to confirm that our developed plating bath could be applied to an enlarged sized membrane. As shown in Table 1, electroless plating of Pd was repeated three times to have thickness of $\sim 6 \mu\text{m}$. The ratio of the plating solution volume to the membrane surface area was $\sim 1.3 \times 10^{-3} \text{ L cm}^{-2}$ and once plating duration was 3 h, i.e., similar with 50.8-mm diameter membrane. This membrane is KIER-Pd-351-20, shown in Table 1. The thickness of the Pd layer was determined to be $\sim 6 \mu\text{m}$ by the weight-gain method. It confirmed that the plating rate on the 88.9-mm diameter substrate was similar to the plating rate of the 50.8-mm substrate. As shown in Fig. 8, the surface of the membrane has a bright palladium color. The KIER-Pd-351-20 membrane has a similar surface color to the KIER-Pd-201-20 membrane made under the same conditions (illumination makes them different). The surface SEM images showed that KIER-Pd-351-20 membrane and KIER-Pd-201-20 membrane had similar morphologies. The cross-sectional SEM image (Fig. 8(c)) confirmed that the membrane thickness was $\sim 6 \mu\text{m}$ like the weight-gain method. The KIER-Pd-351-20 membrane was mounted on a module shown in a previous study [20], and hydrogen permeation tests were performed in a temperature range of 673 to 873 K and a transmembrane pressure difference of 100–500 kPa. The permeation testing results are shown in

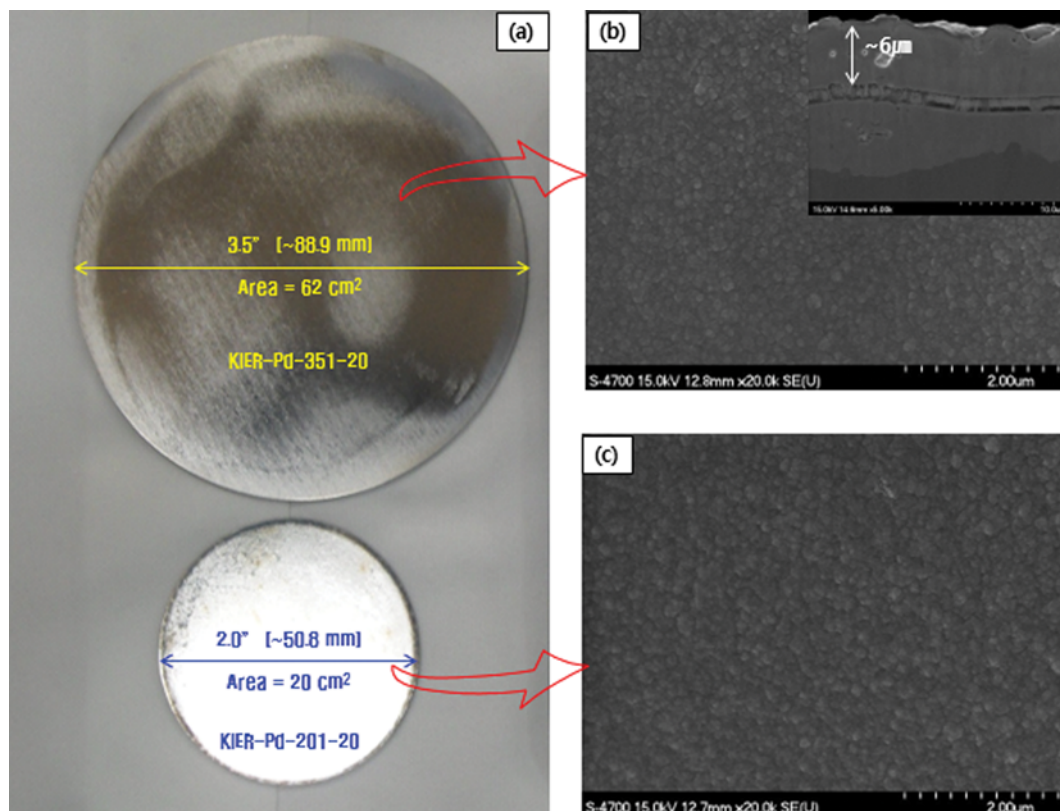


Fig. 8. Photographs of KIER-Pd-201-20 and KIER-Pd-351-20 membranes (a) and surface SEM images of KIER-Pd-351-20 (b) and KIER-Pd-201-20 (c); sub image in (b) is cross-sectional SEM image of KIER-Pd-351-20.

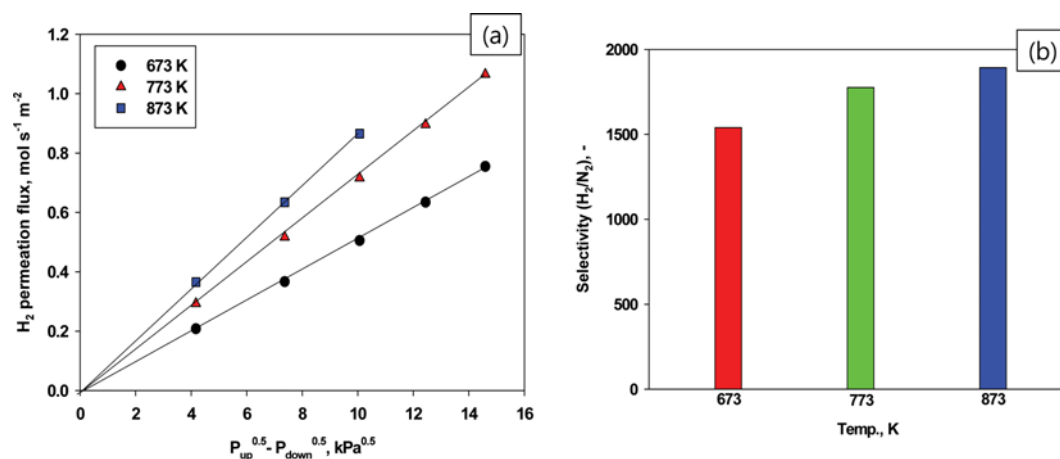


Fig. 9. Hydrogen permeation flux as a function of pressure difference with an exponent of 0.5 (a) and selectivity (H_2/N_2) as a function of temperature at a pressure difference of 100 kPa (b).

Table 2. Comparison of hydrogen permeation behavior between the present membrane and the previous

| Membrane | Thickness [μm] | Temp. [K] | Pressure difference [kPa] | H_2 permeation flux [$\text{mol m}^{-2} \text{s}^{-1}$] | Selectivity [H_2/N_2] | Activation energy [kJ mol^{-1}] | Ref. |
|------------|-----------------------------|-----------|---------------------------|---|---------------------------|--|------------|
| Pd/YSZ/PSS | 7.5 | 773 | 100 | 0.24 | 470 | 12.6 | [18] |
| Pd/YSZ/PSS | 6 | 773 | 100 | 0.29 | 1770 | 13.8 | This study |

Fig. 9. At 873 K and a transmembrane pressure difference of >400 , hydrogen permeation flux was not measured because of the upper limit of the flow meter. As shown in Fig. 9(a), the hydrogen permeation has a good fit with the pressure exponent of 0.5, meaning that the diffusion of hydrogen atom through the Pd layer is rate-limited by Sieverts' law. The hydrogen permeation flux increased with temperature and pressure difference and reached $\sim 0.9 \text{ mol s}^{-1} \text{ m}^{-2}$ at a temperature of 873 K and a pressure difference of 300 kPa. The selectivity between H_2 and N_2 was calculated by the permeation flux ratio measured at a pressure difference of 100 kPa, as shown in Fig. 9(b). The selectivity was $\sim 1,550$ at 673 K, and it reached $\sim 1,850$ at 873 K. Hydrogen permeation behavior between the pre-

vious membrane prepared by the conventional method and the present KIER-Pd-351-20 membrane is compared in Table 2. Considering the thickness, the KIER-Pd-351-20 membrane has similar permeation flux; however, the KIER-Pd-351-20 membrane has much higher selectivity H_2/N_2 . Hydrogen permeation flux through a Pd layer is an activated process, and the activation energy can be obtained from the Arrhenius plot of hydrogen permeance as function of reciprocal temperature. Fig. 10 depicts the Arrhenius plot of the hydrogen permeation through the KIER-Pd-351-20 membrane. The calculated activation energy from the result was $\sim 13.8 \text{ kJ mol}^{-1}$. The activation energy has a dependence on the fabrication method and microstructure or impurities [27], and the reported activation energy is from 5.4 to 38 [28]. As shown in Table 2, the activation energy of the KIER-Pd-351-20 membrane was similar to the previous membrane prepared by the conventional method.

CONCLUSIONS

There are two big issues with the Pd-based composite membrane: thermal stability at high temperature and economical manufacturing. To resolve these issues with the plate-type Pd-based composite membrane, we developed a new plating bath and obtained the following points:

- A new plating bath, which is composed of a holder, a rubber O-ring and a bottom, was successfully substituted for palmitic acid treatment to prevent palladium plating in the pores of the PSS.
- The plating was carried out at a temperature range of 293 to 298 K, which is a comfortable living condition for human beings, so that our ambient temperature plating method provides very simple and economic membrane manufacturing process.

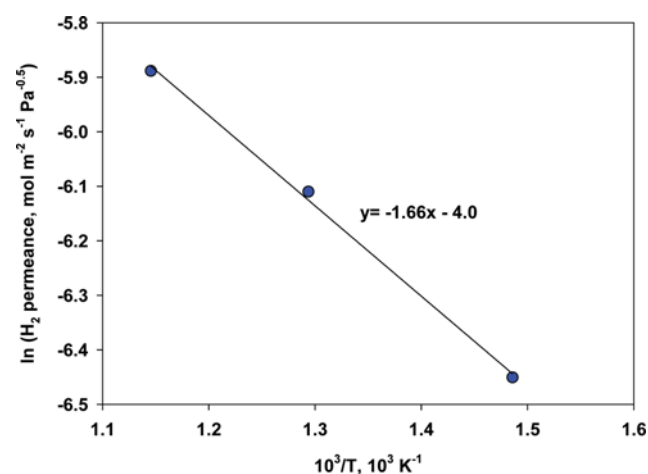


Fig. 10. Arrhenius plot of the hydrogen permeation through the KIER-Pd-351-20 membrane.

- The continuous agitation of the plating solution assisted the transfer of Pd ion and the reducing agent to the membrane surface leading increased plating yield, and ~99.9% of the Pd was plated with our new plating method at ambient temperature. This result means that no Pd recovery process is required before the waste discharge solution.

- A membrane having an 88.9-mm diameter was successfully fabricated. A hydrogen permeation test performed in the range of 673 to 873 K showed that the hydrogen permeation flux reached $\sim 0.9 \text{ mol s}^{-1} \text{ m}^{-2}$ at a temperature of 873 K and a pressure difference of 300 kPa. The selectivity between H_2 and N_2 was $\sim 1,850$ at 873 K and a pressure difference of 100 kPa.

ACKNOWLEDGEMENTS

This work was conducted under the framework of the Research and Development Program of the Korea Institute of Energy Research (KIER) (B6-2449).

REFERENCES

1. M. T. Ravanchi, T. Kaghazchi and A. Kargari, *Desalination*, **235**, 199 (2009).
2. A. Iulianelli and A. Basile, *Catal. Sci. Technol.*, **1**, 366 (2011).
3. M. V. Mundschau, X. Xie, C. R. Evenson IV and A. F. Sammells, *Catal. Today*, **118**, 12 (2006).
4. S. Uemiya, *Sep. Purif. Methods*, **28**, 51 (1999).
5. F. Gallucci, E. Fernandez, P. Corengia and M. V. S. Annaland, *Chem. Eng. Sci.*, **92**, 40 (2013).
6. S. N. Paglineri and J. D. Way, *Sep. Purif. Methods*, **31**, 1 (2002).
7. S. K. Ryi, N. Xu, A. Li, C. J. Lim and J. R. Grace, *Int. J. Hydrogen Energy*, **35**, 2328 (2010).
8. A. Li, W. Liang and R. Hughes, *Catal. Today*, **56**, 45 (2000).
9. M. E. Ayturk and Y. H. Ma, *J. Membr. Sci.*, **330**, 233 (2009).
10. M. Volpe, R. Inguanta, S. Piazza and C. Sunseri, *Surf. Coat. Technol.*, **200**, 5800 (2006).
11. Y. Okinaka and C. Wolowodiuk, Electroless Plating of Platinum Group Metals, in: G. O. Malloy and J. B. Hajdu, *Electroless Plating: Fundamentals And Application*, Reprint Ed., Noyes Publications/William Andrew Publishing, LLC, New York, 421 (1990).
12. K. L. Yeung, R. Aravind, J. Szegner and A. Varma, *Stud. Surf. Sci. Catal.*, **101**, 1349 (1996).
13. B. K. R. Nair, J. Choi and M. P. Harold, *J. Membr. Sci.*, **288**, 67 (2007).
14. K. L. Yeung, S. C. Christiansen and A. Varma, *J. Membr. Sci.*, **159**, 107 (1999).
15. J. N. Keuler, L. Lorenzen and S. Miachon, *Sep. Sci. Technol.*, **37**, 379 (2002).
16. S. Ilias, N.-A. Su, U. I. Udo and F. G. King, *Sep. Sci. Technol.*, **32**, 487 (1997).
17. R. Govind and D. Atneor, *Ind. Eng. Chem. Res.*, **30**, 591 (1991).
18. S.-K. Ryi, S.-W. Lee, D.-K. Oh, B.-S. Seo, J.-W. Park, J.-S. Park, D.-W. Lee and S. S. Kim, *J. Membr. Sci.*, **467**, 93 (2014).
19. S.-K. Ryi, J.-S. Park, K.-R. Hwang, D.-W. Kim and H.-S. An, *Korean J. Chem. Eng.*, **29**, 59 (2012).
20. S.-K. Ryi, C.-B. Lee, S.-W. Lee and J.-S. Park, *Energy*, **51**, 237 (2013).
21. R. Capaccio, Wastewater Treatment For Electroless Plating, in: G. O. Malloy and J. B. Hajdu, *Electroless Plating: Fundamentals And Application*, Reprint Ed., Noyes Publications/William Andrew Publishing, LLC, New York, 519 (1990).
22. M. E. Ayturk and Y. H. Ma, *J. Membr. Sci.*, **330**, 233 (2009).
23. F. Braun, A. M. Tarditi and L. M. Cornaglia, *J. Membr. Sci.*, **382**, 252 (2011).
24. V. K. Bulasara, R. Uppaluri and M. K. Purkait, *Mater. Manuf. Process.*, **27**, 201 (2012).
25. V. K. Bulasara, R. Uppaluri and M. K. Purkait, *Surf. Eng.*, **29**, 489 (2013).
26. P. P. Mardilovich, Y. She and Y. H. Ma, *AIChE J.*, **44**, 310 (1998).
27. T. L. Ward and T. Dao, *J. Membr. Sci.*, **153**, 211 (1999).
28. S.-K. Ryi, J.-S. Park, S.-H. Kim, D.-W. Kim and K.-K. Cho, *J. Membr. Sci.*, **318**, 346 (2008).